2021 43rd Annual International Conference of the
IEEE Engineering in Medicine & Biology Society (EMBC)
Oct 31 - Nov 4, 2021. Virtual Conference

A Cable-actuated Prosthetic Emulator for Transradial Amputees

Souvik Poddar[1], David Cummiskey[1], and Jiyeon Kang[1]

***Abstract*— Upper limb prosthesis has a high abandonment rate due to the low function and heavyweight. These two factors are coupled because higher function leads to additional motors, batteries, and other electronics which makes the device heavier. Robotic emulators have been used for lower limb studies to decouple the device weight and high functionality in order to explore human-centered designs and controllers featuring off-board motors. In this study, we designed a prosthetic emulator for transradial (below elbow) prosthesis to identify the optimal design and control of the user. The device only weighs half of the physiological arm which features two active wrist movements with active power grasping. The detailed design of the prosthetic arm and the performance of the system is presented in this study. We envision this emulator can be used as a test-bed to identify the desired specification of transradial prosthesis, human-robot interaction, and human-in-the-loop control.**

I. INTRODUCTION

Rate of abandonment of bionic limbs to restore the functionality of upper limbs has been considerably high in the amputee population [1]. Studies in the late 19th century reported that lightweight and increased wrist function were one of the most sought after characteristics of a prosthetic arm [2], [3]. Despite the striking technology development in the past few decades, recent studies have highlighted the same demand from prosthesis users [4], [5].

The two most common upper limb prostheses are body-powered (shoulder motion actuated) and myoelectric (surface electromyography actuated) devices for transradial (below elbow) amputees [6]. The widely used transradial prostheses feature only a powered grasping with a fixed wrist. This leads to excessive upper body motion, termed as compensatory motion, affecting also the performance of the intact limb [7], [8]. These compensatory motions have been shown to cause frequent shoulder pain and carpal tunnel syndrome along with other secondary impairments [9], eventually leading to rejection of the bionic arm [7]. In order to address these issues, numerous lightweight transradial prostheses with multi-DoF fingers have been developed [10]–[12]. However, very few studies focused on the multi-DoF functional wrist [13]–[15], despite the important role of the active wrist during daily living tasks. Recently, commercial prosthetic devices that allow for multi-DoF wrist control have been developed [16], [17]. However, these devices weigh about the same as the physiological human arm which is already indicated to be heavy in previous survey studies targeting amputee prosthetic users [1], [18].

[1] is with Mechanical and Aerospace Engineering Department, University at Buffalo, Buffalo 14260, USA (Corresponding email: jiyeonk@buffalo.edu)

The study was partially supported by the SUNY Multidisciplinary Team Grant (RFP 20-02-RSG), 240202-06.

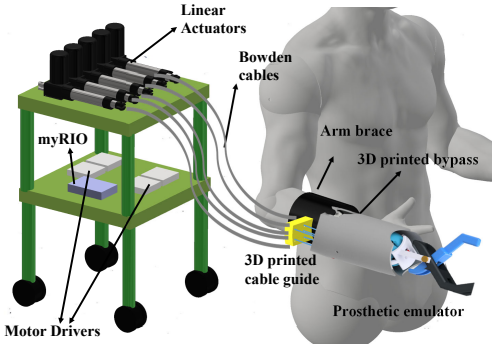

Fig. 1. Concept illustration of the prosthetic device on a subject with off-board electronics setup and bowden cables

Recently, robotic emulators for exoskeleton and prosthesis have been widely adopted to explore different mechanical characteristics of the device or determine optimal parameters such as human-in-the-loop control methods [19], [20]. These emulators feature off-board motors to provide a high capacity of power and minimize the weight that the user needs to carry to decouple the weight and capability of the device. These studies identified the desired parameters while including the user in the decision process of the wearable device [21], [22]. While the user is walking with the device, metabolic cost, EMG, acceleration, heart rate, and center of pressure were observed to determine the parameters of the wearable devices [23], [24]. Unlike the broad studies on the lower limb emulators, there have been limited attempts for the upper limb emulators.

In this study, a cable-actuated prosthetic emulator for the upper limb is designed which features off-board high capacity motors to understand the weight requirement and optimize the wrist DoF of the prosthetic arm which are the most significant factors of prosthetic abandonment (Figure 1). We envision this prosthetic emulator can control the weight and DoF individually which was difficult in previous prosthetic designs. The present study demonstrates an emulator that has less than half the weight of the physiological human arm featuring a 3DOF transradial prosthetic device for pronation/supination, dart-throwing motion, and power grasping. We envision this emulator can be used as a test-bed to alter different mechanical characteristics of the prosthetic arm, develop human-in-the-loop controller, and exploration of various sensory feedback in the future.

II. FUNCTIONAL REQUIREMENTS

In order to perform manipulation tasks for daily living tasks, human uses wrist Pronation/Supination (P/S), Ra-

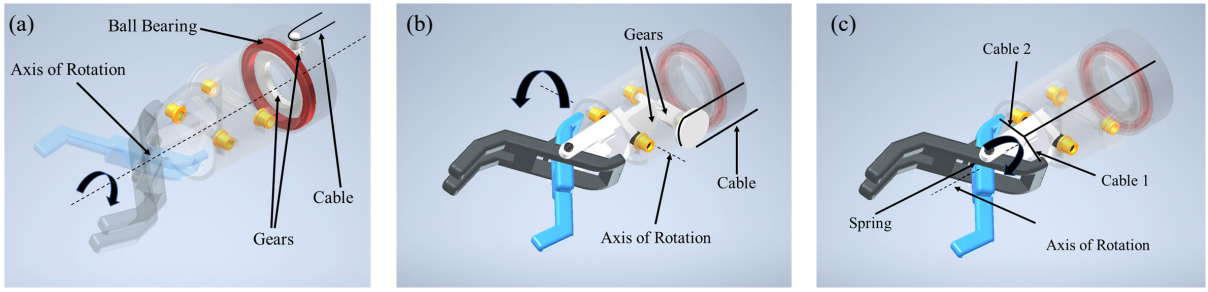

Fig. 2. CAD model illustrations for each degree of freedom depicting actuation mechanism and axis of rotation for (a) Pronation/Supination (b) Dart-throwing motion (c) Power grasping

dial/Ulnar Deviation (R/U), Flexion/ Extension (F/E), and Power Grasping (PG). For optimizing the functionality at the wrist, these four motions were added to the prosthetic device with R/U and F/E combined together to form a Dart-Throwing Motion (DTM) since both of these motions happen almost simultaneously while performing ADLs [25]. The required range of motion corresponding to F/E, R/U, and P/S are 38°/40°, 38°/28°, and 13°/53° respectively with corresponding torques are 0.3 Nm, 0.3 Nm, and 0.06 Nm respectively [13], [26]. Since the prosthetic device is designed to be lightweight, it is envisioned that the overall weight should be less than half of a physiological human arm.

III. Design

The mechanism driving each DOF is made to be simple, compact, and lightweight as shown in Figure 2 satisfying the weight and volume constraints. The P/S motion is driven by a cable, pulley, and bevel gearing mechanism. One of the bevel gears is fixed to a pulley using a cylindrical shaft and the other bevel gear is fixed to the base of the prosthetic device. Rotation of the pulley causes corresponding rotation of the prosthetic device about its rotation axis as shown in Figure 2a. In order to minimize friction, a ball bearing is attached to the base. A gear ratio of 4:1 was used for the bevel gears, while a transmission ratio of 6:1 was used for the pulley connecting the bevel gear, in order to reduce the stroke length required for movements.

The DTM utilizes two spur gears, with a gear ratio of 5:1, which are connected to each other, one of which is fixed to a rotating shaft inside the device and the other is fixed to a setup replicating the wrist containing the fingers. A pulley is attached to the rotating shaft which drives the spur gears causing motion about its corresponding rotation axis, as shown in Figure 2b.

Lastly, the PG is driven by a spring and cable mechanism (Figure 2c). It contains three fingers with their orientation similar to a MyoHand hand from Ottobock [27]. A torsional spring holds the fingers in an open position with a spring rate of 0.58 Nm/360°, making it a voluntary close device. Slots are made in the bottom of the fingers to allow for cables that can be pulled to close the fingers when grasping an object.

To make the device lightweight, the outer frame of the hand, including the fingers and gears, are 3D printed by using lightweight PLA (Polylactic acid) material. The overall weight of the hand is 0.389 kg which is less than half the weight of a human physiological arm. The net volume of the device fits within a 0.1143 $m \times 0.0762$ $m \times 0.2159$ m space. The maximum torques of each DoF are 0.762 Nm, 0.369 Nm, and 0.508 Nm for P/S, DTM, and PG respectively, and corresponding range of motion are -180°to 180°,-25°to 17° and 0° to 53° respectively.

IV. System Assembly

The 3D printed prosthetic device was mounted on an aluminum plate as shown in Fig. 3. In order to drive each degree of freedom, 5 linear actuators (FA-HF-100-12-6, Firgelli Automations, WA) were used having high speed capacity to imitate motions at a broad range of frequencies. Two sets of linear actuators were utilized except power grasping which utilizes a single actuator with a spring. 3D printed mounts made of PLA filaments were developed to hold the actuators onto aluminum frames as shown in the figure. In order to route the cables from the linear actuators to the prosthetic device, bearing pulleys were placed at different positions to minimize friction. Additionally, 3D printed clamps were designed to keep the cable in tension all the way from the prosthetic device to the linear actuators with provisions made for adjusting cable lengths.

V. Control Strategy

To control each degree of freedom, a two-level position-based control strategy using a real-time system MyRio (National Instruments, TX) was developed. The position feedback from the motor is obtained from external potentiometers (FA-LP-5, Firgelli Automations, WA). The high-level control consists of predefined trajectory data obtained from Labview, generated at a frequency of 1000 Hz and position feedback data obtained from a potentiometer. A linear mathematical model was developed to map the voltage from the potentiometer to real-time position. The low-level controller contains a Proportional Integral Derivative (PID) term which tracks the target trajectory by generating Pulse Width Modulation (PWM) pulses that are sent to the motor drivers (AD-MD6321, Firgelli Automations, WA) which control the linear actuators. The PID gains are tuned in accordance with the frequency of motion and degree of

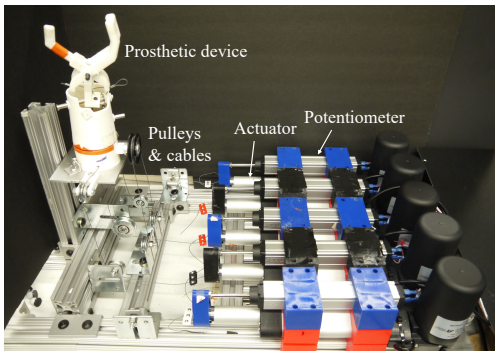

Fig. 3. System assembly containing the prosthetic device, linear actuators, potentiometers, pulleys, and bowden cables mounted on aluminum frames

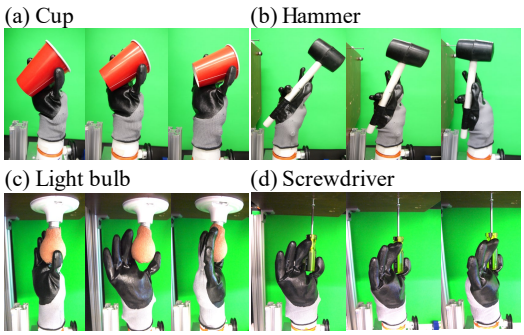

Fig. 4. Demonstration of various ADLs (a) Drinking water from a cup (b) Hammering a nail (c) Screwing in a light bulb (d) Turning a screwdriver

freedom to minimize error between the target and actual trajectories.

VI. Methods

A. Trajectory Tracking and Stability: To analyze the performance of the developed prosthetic device, sinusoidal trajectories were sent to the MyRio controller with a frequency of 0.7 Hz. Reflective markers were placed at different locations on the device to get the measured trajectory from a motion capture system (Vicon, UK). Ten markers were utilized to get trajectories of all the degrees of freedom which includes two for pronation/ supination, four for dart-throwing motion, and four for power grasping. Root Mean Square Errors (RMSE) were calculated for each trial to determine the trajectory tracking performance. To evaluate the stability of the system and determine the speed of motion, step response tests were performed for each degree of freedom. A reference angle in the form of a step command was given for a particular degree of freedom and rise time was calculated until the device positioned itself to the desired angle.

B. Activities of Daily Living (ADLs): Representative tasks were performed using the prosthetic device to demonstrate its feasibility in performing different ADLs. Each activity utilized a particular degree of freedom. Screwing in a lightbulb and turning a screwdriver were chosen to demonstrate P/S. Hammering a nail and drinking a glass of water were chosen to demonstrate DTM. It is noted that the PG movement is utilized in all of the experiments since each ADL involves grasping an object and performing movements.

VII. Result and Discussion

The results obtained from the trajectory tracking are depicted in Figure 5a. The actual angle (black dotted line) is calculated from the reflective markers via a motion capture system as discussed in earlier sections. The desired angle (red solid line) is calculated by taking into account the stroke lengths and transmission factors which include gear ratios and pulley dimensions. The RMSE values obtained for PS, DTM, and PG motion are 4.344°, 2.6173°, and 4.75°, while tracking external sinusoids with frequency at 0.7 Hz and corresponding amplitude at 10°, 10°, and 30° respectively. Therefore, the system shows good performance in tracking external sinusoidal trajectories for pronation/supination, dart-throwing motion, and power grasping, when evaluated with RMSE. Figure 5b shows the results obtained from the step response tests which are performed for each degree of freedom. The rise times recorded for PS, DTM, and PG are 0.44s, 0.18s, and 0.34s for corresponding step input command at 15°, 15°, and 30° respectively, calculated between 10% and 90% of the steady-state (final value). The system showed stable tracking performance for step-response testing. The demonstration of the prosthetic device, covered in a cosmetic glove, while performing different ADLs with intermittent captures is shown in Figure 4. The ADL demonstration shows that the prosthetic device is capable of performing such ADLs and can execute each DOF satisfactorily.

The errors obtained during trajectory tracking can be attributed to multiple factors. One such factor is cable slackening which usually occurs at the extremities of the sinusoidal trajectory as the actuators suddenly change their direction of motion. Another factor is increased friction between different components of the prosthetic device, causing lag in movements. This friction arises due to the motion between pulleys and cables and also among other movable parts of the device like between rotating shafts and fixed bushings that holds the shaft in place.

The emulator developed in this work has a few limitations. It is yet to be explored for use in off-board settings for which a number of design modifications have to be made. Due to the limited speed capacity of the current actuators, the emulator is limited in its use to a fixed range of frequencies. This also limits its ability to perform ADLs which require high torque, force, and speed requirements like throwing a ball to a far distance or performing motion with heavy objects. In the future, the implementation of a more efficient controller will be carried out to reduce the RMSE errors between desired and actual trajectories. This can be done by optimizing the PID gains associated with the control architecture. More efficient design and mechanisms will be explored for all the degrees of freedom. Methods to reduce manufacturing errors and friction between components will be investigated. In addition, off-board use of the prosthetic device with healthy and amputee participants will be tested. Studies involving ADLs will be conducted to determine the efficacy of the

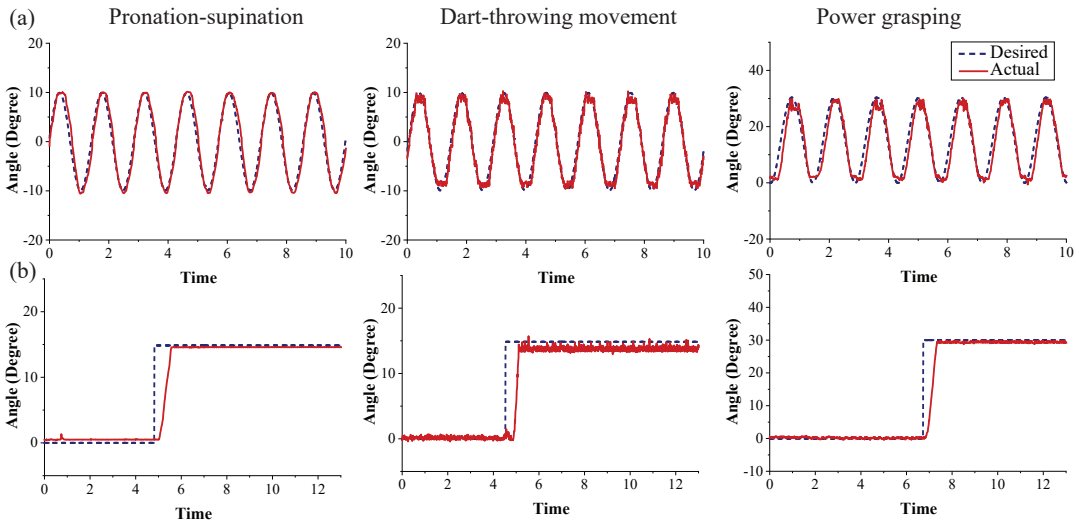

Fig. 5. Performance evaluation of the cable-actuated prosthetic device (a) Tracking sinusoidal inputs at 0.7 Hz (b) Step response of Stability tests

prosthetic device by integrating Electromyography (EMG) and IMU sensors as control inputs and test the feasibility with participants to evaluate the movement quality of ADL activities.

REFERENCES

[1] E. Biddiss and T. Chau, "Upper limb prosthesis use and abandonment: a survey of the last 25 years," *Prosthetics and orthotics international*, vol. 31, no. 3, pp. 236–257, 2007.

[2] D. J. Atkins, D. C. Heard, and W. H. Donovan, "Epidemiologic Overview of Individuals with Upper-Limb Loss and Their Reported Research Priorities," *Journal of Prosthetics and Orthotics*, vol. 8, no. 1, pp. 2–11, 1996.

[3] P. J. Kyberd, D. J. Beard, J. J. Davey, and D. J. Morrison, "A survey of upper-limb prosthesis users in oxfordshire," *Journal of Prosthetics and Orthotics*, vol. 10, no. 4, pp. 84–91, 1998.

[4] L. Resnik, M. Borgia, and M. Clark, "A National Survey of Prosthesis Use in Veterans with Major Upper Limb Amputation: Comparisons by Gender," *PM&R*, 2020.

[5] B. Stephens-Fripp, M. Jean Walker, E. Goddard, and G. Alici, "A survey on what Australians with upper limb difference want in a prosthesis: justification for using soft robotics and additive manufacturing for customized prosthetic hands," *Disability and Rehabilitation: Assistive Technology*, vol. 15, no. 3, pp. 342–349, 2020.

[6] J. Kang, M. A. Gonzalez, B. Gillespie, and D. Gates, "A haptic object to quantify the effect of feedback modality on prosthetic grasping," in press, *IEEE Robot. Autom. Lett.*, 2019.

[7] A. Metzger, A. Dromerick, R. Holley, and P. Lum, "Characterization of compensatory trunk movements during prosthetic upper limb reaching tasks," *Archives of physical medicine and rehabilitation*, vol. 93, no. 11, pp. 2029–2034, 2012.

[8] A. Mell, B. Childress, and R. Hughes, "The effect of wearing a wrist splint on shoulder kinematics during object manipulation," *Archives of Physical Medicine and Rehabilitation*, vol. 86, no. 8, pp. 1661–1664, 2005.

[9] H. Burger and G. Vidmar, "A survey of overuse problems in patients with acquired or congenital upper limb deficiency," *Prosthetics and orthotics international*, vol. 40, no. 4, pp. 497–502, 2016.

[10] J. Fajardo, V. Ferman, D. Cardona, G. Maldonado, A. Lemus, and E. Rohmer, "Galileo hand: An anthropomorphic and affordable upper-limb prosthesis," *IEEE Access*, vol. 8, pp. 81 365–81 377, 2020.

[11] W. Ryu, Y. Choi, Y. J. Choi, Y. Lee, and S. Lee, "Development of an anthropomorphic prosthetic hand with underactuated mechanism," *Applied Sciences*, vol. 10, no. 12, p. 4384, 2020.

[12] E. Hocaoglu and V. Patoglu, "Design, implementation and evaluation of a variable stiffness transradial hand prosthesis," *CoRR*, vol. abs/1910.12569, 2019.

[13] C. Semasinghe, R. Ranaweera, J. Prasanna, H. Kandamby, D. K. Madusanka, and R. Gopura, "Hypro: A multi-dof hybrid-powered transradial robotic prosthesis," *Journal of Robotics*, vol. 2018, 2018.

[14] V. Abarca, K. Flores, and D. Elías, "The octa hand: An affordable multi-grasping 3d-printed robotic prosthesis for transradial amputees," in *2019 5th International Conference on Control, Automation and Robotics (ICCAR)*. IEEE, 2019, pp. 92–97.

[15] Y. Nemoto, K. Ogawa, and M. Yoshikawa, "F3hand ii: A flexible five-fingered prosthetic hand using curved pneumatic artificial muscles," in *2020 IEEE/SICE International Symposium on System Integration (SII)*. IEEE, 2020, pp. 99–104.

[16] ottobockus, "Michelangelo prosthetic hand," Available at https://www.ottobockus.com/prosthetics/upper-limb-prosthetics/solution-overview/michelangelo-prosthetic-hand/.

[17] ossur, "i-limb," Available at https://www.ossur.com/en-us/prosthetics/arms/i-limb-ultra.

[18] S. Plagenhoef, G. Evans, and T. Abdelnour, "Anatomical data for analyzing human motion," *Research quarterly for exercise and sport*, vol. 54, no. 2, pp. 169–178, 1983.

[19] S. Collins, Bruce Wiggin, and G. Sawicki, "Reducing the energy cost of human walking using an unpowered exoskeleton," *Nature*, vol. 522, no. 7555, pp. 212–215, 2015.

[20] M. Kim, Y. Ding, P. Malcolm, J. Speeckaert, C. Siviy, C. Walsh, and S. Kuindersma, "Human-in-the-loop bayesian optimization of wearable device parameters," *PloS one*, vol. 12, no. 9, p. e0184054, 2017.

[21] J. Zhang, P. Fiers, K. Witte, R. Jackson, K. Poggensee, C. Atkeson, and S. Collins, "Human-in-the-loop optimization of exoskeleton assistance during walking," *Science*, vol. 356, no. 6344, pp. 1280–1284, 2017.

[22] W. Felt, J. Selinger, M. Donelan, and D. Remy, "" body-in-the-loop": Optimizing device parameters using measures of instantaneous energetic cost," *PloS one*, vol. 10, no. 8, p. e0135342, 2015.

[23] V. Chiu, A. Voloshina, and S. Collins, "An ankle-foot prosthesis emulator capable of modulating center of pressure," *IEEE Transactions on Biomedical Engineering*, vol. 67, no. 1, pp. 166–176, 2019.

[24] K. Ingraham, E. Rouse, and D. Remy, "Accelerating the estimation of metabolic cost using signal derivatives: Implications for optimization and evaluation of wearable robots," *IEEE Robotics & Automation Magazine*, vol. 27, no. 1, pp. 32–42, 2019.

[25] V. Vardakastani, H. Bell, S. Mee, G. Brigstocke, and A. E. Kedgley, "Clinical measurement of the dart throwing motion of the wrist: variability, accuracy and correction," *Journal of Hand Surgery (European Volume)*, vol. 43, no. 7, pp. 723–731, 2018.

[26] J. C. Perry, J. Rosen, and S. Burns, "Upper-limb powered exoskeleton design," *IEEE/ASME transactions on mechatronics*, vol. 12, no. 4, pp. 408–417, 2007.

[27] ottobockus, "Myohand," Available at https://www.ottobockus.com/prosthetics/upper-limb-prosthetics/solution-overview/myoelectric-devices-speedhands/.